FINITE ELEMENT ANALYSIS OF COMPOSITE STRUCTURES WOUND BY WIDE PLIES.

J.-P. Jeusette (a), G. Laschet (b) and S. Idelsöhn (c)

ABSTRACT

An isoparametric axisymmetrical finite element is developed for the analysis of multilayer composite structures wound by wide plies. This element takes into account the variation of angle along the width of a layer, i.e., along a given parallel between two meridian lines of a revolution structure. Evaluation of strain and stress tensors is performed in mean fiber and in extreme fibers directions of a ply; so, those extreme values give bounds of a trust interval centered on the mean direction values obtained with a classical element, presenting a constant filament direction along the width of the ply, the relative difference between stresses in mean and extreme directions can reach 20%! Moreover, the model can represent geometrical nonlinear behaviour and material nonlinearities. The influence of the variation of angle on the intralaminar degradation onset is described and different choices of degradation factors are compared on a model of a real wound structure.

(a) Research fellow of CONICET, from Aerospace Laboratory of the University of Liège, Belgium.
(b) Research engineer - Aerospace Laboratory of the University of Liège, Belgium.
(c) Scientific and Technological Research staff member of CONICET.

INTRODUCTION

The winding technology has application in the domain of aerospace structures as motor cases of launchers and missiles which need an exceptional resistance/weight ratio. Other applications are investigated in the marine activities (offshore petroleum structures, ...) [1,2]. Thus, it seems very important to understand the behaviour of such structures.

Actually, some manufactures wind structures with wide layers. This kind of winding process constitutes an economical and mechanical interest. But, in extreme structure's regions, fibers of a layer, make with the meridian line, an angle which changes on a given parallel.

The paper's purpose consists in developing a finite element formulation for analysis of multilayer composite materials, taking into account this variation of angle along the width of a ply. This finite element, representing geometrical nonlinear behaviour and material nonlinearities, is very useful to study wound structures; indeed, such structures are formed with multidirectional composite for which intralaminar degradation process occurs before delamination [3,4].

After having presented, in the first section, a basic description of a wound composite structure, some theoretical assumptions of the finite element model are described in the second one and the degradation models in a third section.

The effects of the variation of angle on the degradation process are described in section fourth. Finally, different choices of degradation onset are applied on an academic application; we also compare, on a real wound structure (a spherical motor case of missile), the results given by our new method to results obtained with the classical element, having a constant filament direction along the width of a ply.

1. Description of a Wound Composite Structure

Generally, wound composite structures are cylinders having two axisymmetrical rings at their extremities. They are manufactured with a metallic liner wrapped by wound composite layers. The liner is used as a mandrel during the manufacturing process, insures gastightness and provides also a small amount of the mechanical strength [2].

An example of a wound structure is shown in Fig. 1. Only a quarter of the whole wound tank is presented: the z-axis is the revolution one and the plane oxy constitutes the equatorial plane of the ring (extreme part of the structure); the curve (I) represents the trajectory of a fiber on tank's surface: near the opening's region (maximum value of z-coordinate), (I) has to be tangent to the last parallel.

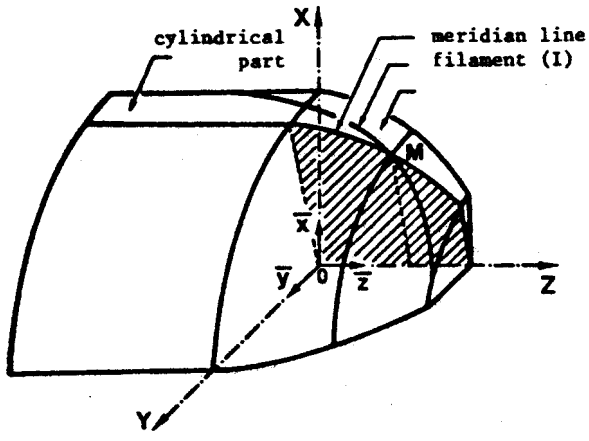

Fig. 1: wound axisymmetrical tank
- cylindrical part
- extreme ring with openings

In the polar zone, near the gap of the ring, there is local increasing of composite thickness because the plies have to be bent for going on the winding. This region is critical when internal pressure grows because of important local flexions. Fig. 2 illustrates the thickness profile of composite material wound on a sphere.

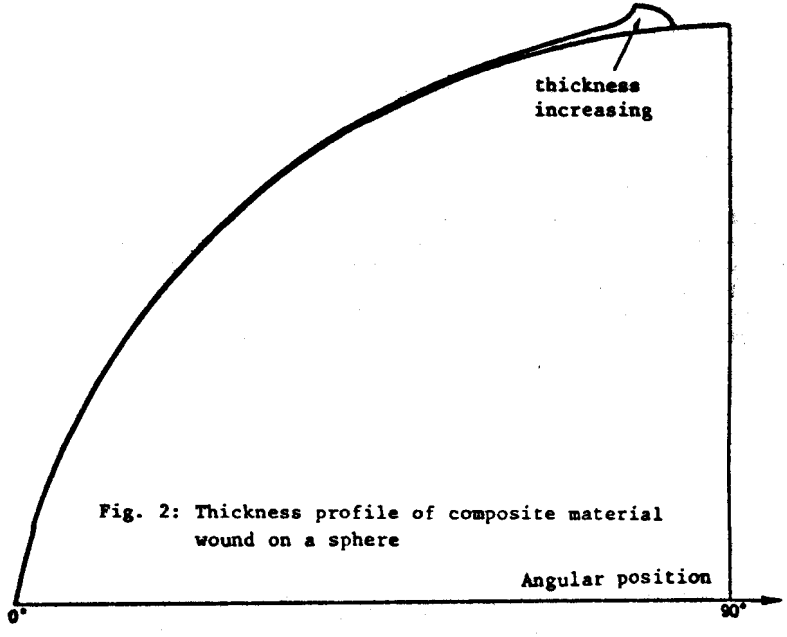

Fig. 2: Thickness profile of composite material wound on a sphere

To extenuate this effect (i.e., to spread the local "bubble" in the thickness profile of Fig. 2) and to decrease the winding time, some manufactures wind structures with wide layers (for example, the ratio, width of the ply to radius of cylinder, can be equal to 0.05). But the width of plies influences mechanical properties of composite material, which is still orthotropic in a global way. In fact, as shown in Fig. 3, in extreme structure's regions, filaments of a layer, make with the meridian line, an angle which changes on a given parallel. One assumes that fibers are distributed in an interval $[\alpha_1,\alpha_2]$. To keep axisymmetrical properties of the structure, symmetrical filaments are setting inside interval $[-\alpha_2,-\alpha_1]$.

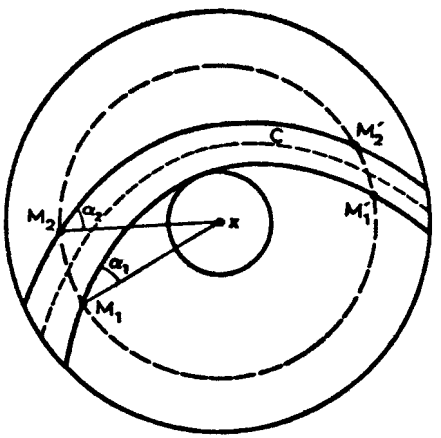

Fig. 3: Variation of angle along the width of a layer (M_1M_2), on a given parallel of a revolution structure with extreme gaps.

x : revolution axis perpendicular to paper
o : trajectory of half-width fiber of the ply

The difference of angles along the width of a ply can reach 50 degrees near the polar zones of the structure! Thus, it seems important taking into account this effect to evaluate failure criteria because polar regions are often critical. In the Fig. 4, one can see evolution of angle fiber/meridian line along a surface's meridian line of a spherical tank (as in Fig. 3) with opening at a latitude angle of 85 degrees. For this case, the width of a layer is 10 millimeters; at the equatorial plane, all angles are equal to 6.3 degrees. The four curves represent angles at the edges of a ply (α_1 and α_2) , the angle at half width (dashed curve) and the mean angle $(\alpha_1+\alpha_2)/2$. The two last angles differ only in the polar zone; there, the curve of mean angle tends to the curve of α_2 just when α_1 reaches its maximum value (90 degrees).

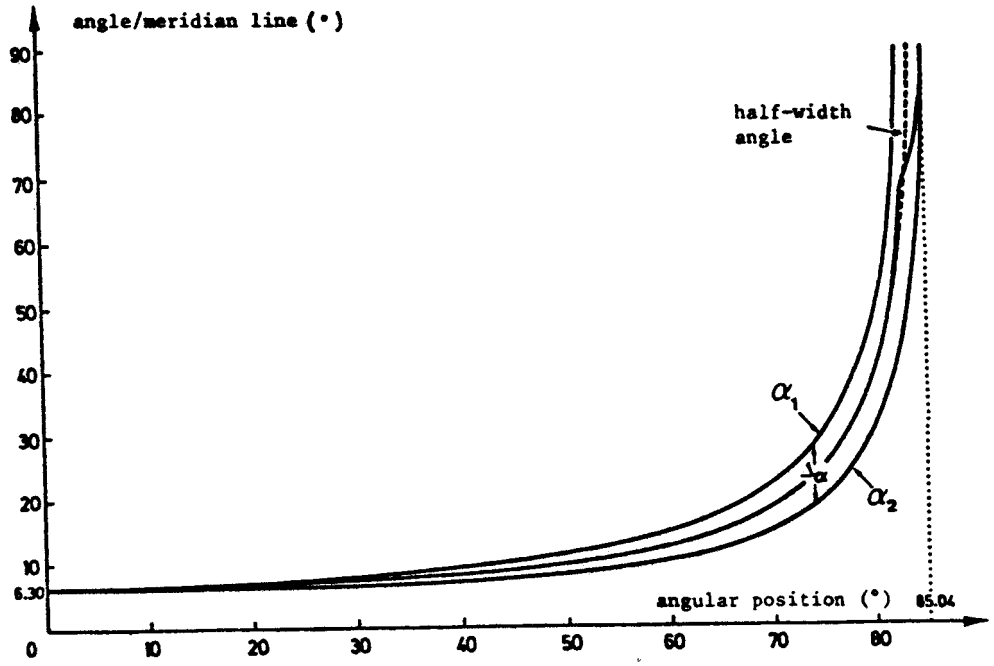

Fig. 4: Evolution of angles along a surface's meridian line of a spherical tank with openings at a latitude angle of 85 degrees

2. Finite Element Model

The model used consists of an isoparametric, axisymmetrical displacement finite element as basic element. We can use one element per layer discretization: like that, each ply has its own displacement field. In the other part, one can postulate a unique displacement field for several plies; in this case, the stiffness matrix is obtained by summing the contribution of each layer, using the same field for the whole element which becomes a multilayer element. The total number of degrees of freedom of the element is then independent of the number of layers. [6]

Orthotropic stress-strain relations are introduced for each ply. These stress-strain relations may be linear, nonlinear or multilinear before degradation of material matrix. In addition, two different stress-strain relations are adopted for the post-degradation behaviour. The matrix and fibers degradations are governed by failure criteria as TSAI-HILL's, TSAI-WU's and SANDHU's ones.

This kind of finite element is very useful to study wound structures; indeed, such structures are formed with multidirectional composite for which degradation occurs before delamination. The model, based on displacement assumptions, also includes geometrical nonlinearities [3].

The structural axis $(\vec{E}_r,\vec{E}_\theta,\vec{E}_z)$ of element, local axis $(\vec{e}_x,\vec{e}_y,\vec{e}_z)$ and orthotropic axis $(\vec{e}_1,\vec{e}_2,\vec{e}_3)$ of a ply are shown in Fig. 5.

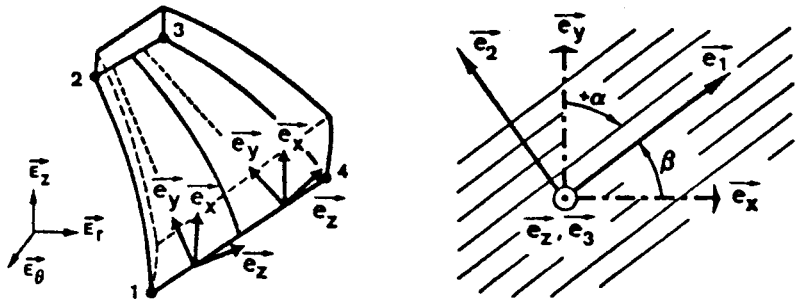

Fig. 5: Structural $(\vec{E}_r,\vec{E}_\theta,\vec{E}_z)$, local $(\vec{e}_x,\vec{e}_y,\vec{e}_z)$ and orthotropic $(\vec{e}_1,\vec{e}_2,\vec{e}_3)$ axis systems

This element takes into account a variation of angle along the width of a ply. To keep economical advantages of an axisymmetrical study, we had to do some geometrical and material properties assumptions [4].

In the material properties part:

- in the case of wound structures, a given parallel is crossed by filaments of angle $(+\alpha)$ when the ply passes and fibers of angle $(-\alpha)$ when the same ply comes back, that for the case of constant angle; so, the structure is globally orthotropic; to approach the real structure, and, in the same time, to conserve material symmetry, one assumes that each layer (α) of an element is formed by two sublayers $(\pm\alpha)$, having the same thickness; so, the Hooke matrix, defined in (2.1), keeps, along a whole parallel, its orthotropic properties in the local axis system reported in Fig. 5,

$$H = \frac{H(+\alpha) + H(-\alpha)}{2} \qquad (2.1)$$

where $H(+\alpha)$ is the Hooke matrix, in the local axis system of sublayer $(+\alpha)$; $H(+\alpha)$ and $H(-\alpha)$, taken separately, don't have an orthotropic form.

In the geometrical part:

- as shown in Fig. 6, the variation of angle is assumed to be linear between α_1 and α_2 values, along the width of a ply:

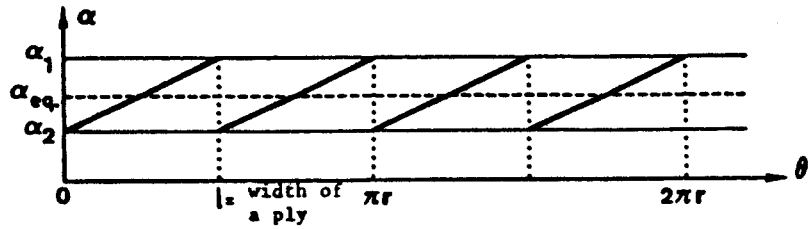

Fig. 6: Linear variation of angle along the width of a ply

- an equivalent layer, having the same thickness that the real one, contains filaments in an uniform equivalent direction; graphical interpretation of equivalent angle is represented in Fig. 7; this angle is the same for all other plies along the parallel (Fig. 6), then geometrical axisymmetry is respected.

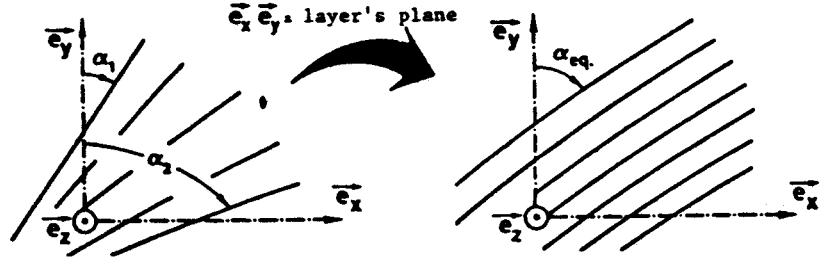

Fig. 7: Variation of angle and equivalent angle in the layer's plane

We can apply the precedent suppositions to layers presenting variation of angle along the width on a given parallel. For taking into account this change, one should have to calculate an equivalent Hooke matrix summing the contributions of all directions of fibers, so:

$$H_{eq} = \frac{\int_{\alpha_1}^{\alpha_2} [H(+\alpha) + H(-\alpha)]\, d\alpha}{2\,(\alpha_2-\alpha_1)} \qquad (2.2)$$

where α_1 and α_2 are limits of the variation of angle on a ply.

We can easily show that expression (2.2) can be reduced with good approximation to:

$$H_{eq} = \frac{H(+\alpha_{eq}) + H(-\alpha_{eq})}{2\,(\alpha_2-\alpha_1)} \qquad (2.3)$$

with α_{eq}, the arithmetic mean angle $(\alpha_1+\alpha_2)/2$ of the two extreme angles.

To verify strength of a layer, failure criteria are evaluated with stresses calculated in the direction of mean filament and in the direction of extreme fibers of the ply. The used criteria are valid for orthotropic plies. Thus, all those quantities are evaluated on assuming orthotropic material properties in each direction (mean and extreme). We can imagine that the real layer is composed by three thin plies having filaments respectively at constant α_1, α_2 and $(\alpha_1+\alpha_2)/2$ angles. Obviously, those three thin plies could be discretizated explicitely but this model should be more expensive and, moreover, problem of selecting right thicknesses persists.

Stresses in the three orthotropic directions are obtained by (2.4); Fig. 8 illustrates the axis system;

$$\begin{aligned} &\cdot\ \underset{\sim}{\sigma}_{\alpha m} = \underset{\approx}{H}_{or}\ \underset{\sim}{\varepsilon}_{\alpha m} \\ &\cdot\ \underset{\sim}{\sigma}_{\alpha 1} = \underset{\approx}{H}_{or}\ \underset{\sim}{\varepsilon}_{\alpha 1} = \underset{\approx}{H}_{or}\ \underset{\approx}{R}^{*-1}(\gamma)\ \underset{\sim}{\varepsilon}_{\alpha m} \\ &\cdot\ \underset{\sim}{\sigma}_{\alpha 2} = \underset{\approx}{H}_{or}\ \underset{\sim}{\varepsilon}_{\alpha 2} = \underset{\approx}{H}_{or}\ \underset{\approx}{R}^{*}(\gamma)\ \underset{\sim}{\varepsilon}_{\alpha m} \end{aligned} \qquad (2.4)$$

with $\underset{\approx}{R}^{*}$, a rotation matrix from $\vec{e}_{1m}$ to $\vec{e}_{12}$ with an angle γ equal to $(\alpha_2-\alpha_1)/2$;
with $\alpha_m = (\alpha_1+\alpha_2)/2$.

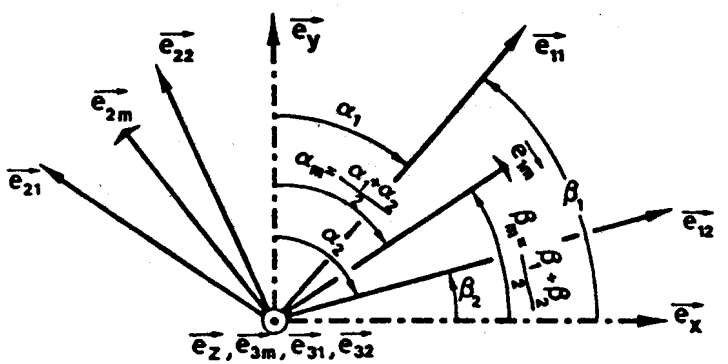

Fig. 8: Local axis system $(\vec{e}_x, \vec{e}_y, \vec{e}_z)$.
Orthotropic axis systems $(\vec{e}_1, \vec{e}_2, \vec{e}_3)$
for the three directions.

Stresses are calculated in the sub-layer $(+\alpha_1, +\alpha_2, +\alpha_m)$; indeed, in sub-layers $+\alpha_1$ and $-\alpha_1$, normal stresses have the same values; only shear stresses have opposite signs. Then, to be consistent, one has to assume that stiffness and failure limits are the same for positive and negative shear; it's a limitation of this model.

So, the extreme stresses ($\underset{\sim}{\sigma}_{\alpha 1}$ and $\underset{\sim}{\sigma}_{\alpha 2}$) gives bounds of a trust interval centered on the mean stresses ($\underset{\sim}{\sigma}_{\alpha m}$) ; the stresses $\underset{\sim}{\sigma}_{\alpha m}$ can also be obtained by a classical model of an orthotropic ply showing

fibers at a constant angle $\alpha = \alpha_m$; indeed, the corresponding equivalent Hooke matrix is calculated with angle α_m . We can remark that extreme stresses evaluated by mean stresses rotation, are not referred to orthotropic axis system and thus, cannot be used in failure orthotropic criteria.

3. Description of Material Behaviour [3]

a) Behaviour before matrix degradation

- linear elastic material which is an Hookean model;
- nonlinear material; when, for a given stress state, the matrix plays an important role, the behaviour of composite becomes nonlinear (often, experimental transversal and shear stress-strain relations are nonlinear); here, an incremental model due to Sandhu is adopted which takes into account the multiaxial strain state;
- material with different moduli in tension and compression; uniaxial stress-strain relations are approximated by a bilinear representation and the choice of stress-strain matrix components differs when stress components are in tension or in compression.

b) Failure criteria

Failure criteria are introduced to model the nonlinear behaviour due to partial degradation (i.e., matrix degradation) and to represent ply-by-ply progressive failure in composite materials. The average stress components are used to check whether criterion is verified or not.

- Tsai-Hill criterion states that the matrix degradation is reached in the orthotropic directions of a layer when

$$f(\sigma) = F(\sigma_2-\sigma_3)^2 + G(\sigma_3-\sigma_1)^2 + H(\sigma_1-\sigma_2)^2 + 2L\,\tau_{23}^2 + 2M\,\tau_{31}^2 + 2N\,\tau_{12}^2 = 1$$

  where F,G,H,L,M,N are formed with ply's tensile and shear strengths.

- Tsai-Wu criterion which takes into account the different stress limits in tension and in compression

$$f(\sigma) = F_i\,\sigma_i + F_{ij}\,\sigma_i\,\sigma_j = 1 \qquad i,j = 1,\ldots,6$$

  where F_i , F_{ij} are respectively vector and tensor components formed by tensile, compressive and shear strengths.

- Sandhu criterion, based on the concept that strain energies under longitudinal, tranverse and shear loadings are independent parameters, can be written as

$$\sum_{i=1}^{3}\sum_{j=1}^{3}\left[\left(\int_{\varepsilon_{ij}^{eq}} \sigma_{ij}\, d\varepsilon_{ij}^{eq}\right)/K_{ij}\right] \qquad (3.1)$$

  where ε_{ij}^{eq} are the equivalent strains taking into account the multiaxial strain state and K_{ij} are the failure principal strain energies under uniaxial tension and compression.

c) Post-degradation behaviour

After matrix degradation of a layer, transverse and shear stiffness decrease to a small value; only the elastic modulus in the filament direction is preserved. However, in wound composite materials, the degraded elastic and shear moduli are not negligible. We retain two

possibilities for our case:

- the tranverse and shear stresses in a degraded ply are assumed to be maintained at their value; that means

$$\underset{\sim}{\sigma} = \underset{\sim}{\sigma}^* + \underset{\approx}{H}_d(\underset{\sim}{\varepsilon}-\underset{\sim}{\varepsilon}^*) \quad \text{where} \quad \underset{\approx}{H}_d = \begin{bmatrix} E_{11} & & & & & 0 \\ & E_d & & & & \\ & & E_d & & & \\ & & & G_d & & \\ & & & & G_d & \\ 0 & & & & & G_d \end{bmatrix}$$

where $\underset{\sim}{\sigma}^*$ and $\underset{\sim}{\varepsilon}^*$ are the stresses and strains at degradation, with E_{11}, elastic modulus in the fiber direction, E_d, E_g, tranverse and shear moduli after degradation;

- the tranverse and shear stresses in the degraded ply decrease linearly from the failure value to zero in such a way that the failure principal strain energies (K_{ij}) keep the same value (Fig. 9).

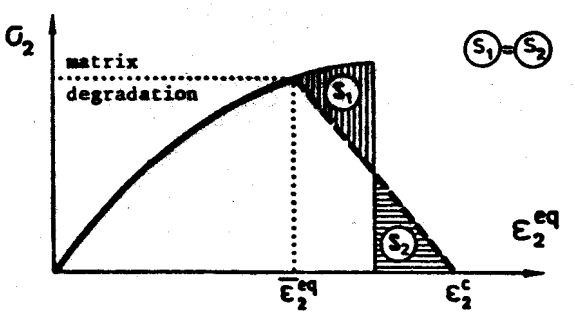

Fig. 9: Post-degradation model

d) Failure criteria for total degradation

When the longitudinal stress reaches a critical value, the fibers break; all stresses are relaxed and are carried out by the neighbouring layers. The value is

- for Tsai-Hill, $$(\sigma_{11}/x_1^t)^2 = 1 \qquad (3.2)$$

- for Tsai-Wu, $$F_1\,\sigma_{11} + F_{11}\,\sigma_{11}^2 = 1 \qquad (3.3)$$

with $$F_1 = \frac{1}{X_1^t - X_1^c} \quad ; \quad F_{11} = \frac{1}{X_1^t\,X_1^c}$$

where X_1^t, X_1^c are longitudinal tensile and compressive strengths;

- for Sandhu, $$\varepsilon_1^{eq} = \varepsilon_1^f \qquad (3.4)$$

with ε_1^f , the failure strain in a uniaxial longitudinal test.

4. Effect of Variation of Angle on Degradation Process

The Newton-Raphson method is used to solve the nonlinear problem. When implementing this algorithm, the correct integration of the constitutive equations (4.1) in the presence of multimodulus material or during the matrix degradation is performed [3]:

$$\Delta\sigma_k = \int_{\Delta\varepsilon_k} C_{(\sigma,\varepsilon)}\, d\varepsilon \qquad (4.1)$$

for iteration k of an increment.

a) in N-linear problem

If the matrix degradation is reached in any point of the structure, the stress increment is written,

$$\Delta\sigma = \sum_{i=1}^{N} C_i(\sigma_i,\varepsilon_i)\, \Delta\varepsilon_i$$

where N is the number of stress-strain relation changes during an iteration of Newton-Raphson algorithm. To evaluate $\Delta\varepsilon_i$, a factor r_i is calculated at each step so that $r_i\, \Delta\varepsilon$ $(= \Delta\varepsilon_i)$ is the part necessary to reach a discontinuity point as degradation.

In fact, r_i is the factor by which one has to multiply the increment of stresses $(\Delta\sigma)$ to reach degradation (i.e., to verify failure criteria), see (4.2),

$$F(\sigma^* + r_i\, \Delta\sigma) = 1 \qquad (4.2)$$

where σ^* is the stress state at precedent iteration and F is the function of Tsai-Hill or Tsai-Wu.

In a composite structure wound by wide plies, we have informations about strains and stresses in mean filament and extreme fibers directions of a layer. Calling r_{am} , r_{a1} , r_{a2} the degradation factors evaluated respectively with $\Delta\sigma_{\alpha m}$, $\Delta\sigma_{\alpha 1}$, $\Delta\sigma_{\alpha 2}$ ($\Delta\sigma_{\alpha 1}$ and $\Delta\sigma_{\alpha 2}$ as in formula 2.4), we use a factor r_i function of r_{am} , r_{a1} and r_{a2} to decree matrix degradation of a ply; indeed, only alone degradation decision can be taken by ply (to take three independent decisions, three different orthotropic layers should have to be used). Taking into account that stresses in extreme directions give bounds on stresses existing in the layer, we propose three different choices to decree matrix degradation:

- $r_i = r_m$; like that, the behaviour of a ply is governed by the behaviour in the mean direction; if, for example, failure criterion is verified in direction α_1 , local degradation is met but, with this choice, the stiffness matrix is unchanged because there is still strength in α_m direction;

- $r_i = Ar_{a1} + Br_{am} + Cr_{a2}$; this combined factor takes into account the variation of angle along the width of a ply; Fig. 10 gives a graphical interpretation of choice for those constants A, B and C; we assume that those influence curves are formed with parabolic functions so that $A = C = 0.125$ and $B = 0.75$; the hatching area in Fig. 10 represents region of dominant effect of r_{am} ;

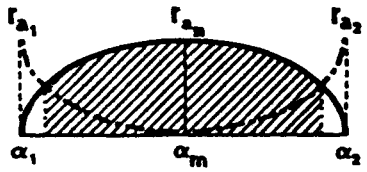

Fig. 10. Influence curves of degradation factors.

- $r_i = \min (r_{am}, r_{a1}, r_{a2})$; like that, we have the best security with respect to the degradation onset; when stresses, in one of the three directions, verify failure criterion, one decrees degradation and changes stiffness matrix.

After matrix degradation of a layer, fibers have to support the most important part of load until longitudinal stress component reaches failure limit. As for the case of matrix degradation, we define parameters K_m , K_{a1} , K_{a2} evaluated respectively with $\sigma_{\alpha m}11$, $\sigma_{\alpha 1}11$ and $\sigma_{\alpha 2}11$ (see relations 3.2 and 3.3). To decree filaments break or total degradation of a ply, three choices can still be made:

$$- K = K_m$$

$$- K = A K_{a1} + B K_m + C K_{a2} \qquad (4.3)$$

$$- K = \max (K_m , K_{a1} , K_{a2})$$

b) Nonlinear material problems

In this case, total strain increment is subdivided into m sufficiently small parts and the total stress increment is evaluated by Euler's explicit integration. So, it's easy to verify when matrix degradation occurs [3]. Here, stresses in the extreme fibers directions (α_1 and α_2) are obtained, from stress-strain uniaxial curves, by rotating equivalent strain tensor of the Sandhu model ($\varepsilon^{eq}_{\alpha m}$) . Matrix degradation factors can be determined with criterion (3.1); the total layer degradation is governed by criterion (3.4) based on failure strains $\varepsilon^f_{\alpha m}11$, $\varepsilon^f_{\alpha 1}11$ and $\varepsilon^f_{\alpha 2}11$; after matrix degradation, as deformation modes are independent, ε^{eq} equals to the real strain ε . The three choices for decreing matrix degradation or filaments break are the same that in N-linear problem.

5. Numerical Results

a) Axisymmetrical cylinder

To compare classical multilayer element to element developed here,

a simple composite cylinder, submitted to a radial load at the end, was examined.

The structure is modeled by three elements in axial and radial directions (Fig. 11). We used two models:

- each element contains three classical layers having fibers directions at constant angles of 75°, 82.5° and 90° with respect to axial direction (curve 1 in Fig. 12);
- each element is formed with a ply presenting a variation of angle $\Delta\alpha = 15°$ with extreme filaments directions α_1 and α_2 equal to 75° and 90°; the three choices of degradation factors of section 4. are used, i.e., mean factor (curve 2 in Fig. 12), combined factor (curve 3 in Fig. 12) and minimum factor (curve 4 in Fig. 12).

The mechanical properties of layers in wound glass-epoxy composite material before degradation are (the material behaviour is assumed to be linear before degradation):

$$E_1 = 5810 \text{ hb.} \quad , \quad E_2 = E_3 = 1687 \text{ hb.}$$

$$G_{12} = G_{13} = G_{23} = 787 \text{ hb.}$$

$$\nu_{12} = \nu_{13} = \nu_{23} = 0.278$$

The Tsai-Wu failure criterion is used; strengths are

- in the fiber direction : X = 105 hb;
- in tranversal directions : Y = Z = 7 hb;
- for shear : R = S = T = 5 hb;
- for shear at 45° of fiber : U = V = W = 7.5 hb.

After matrix failure of a layer, transversal and shear stresses are assumed to be maintained at their values of degradation; tranversal and shear moduli are reduced to

$$E_d = 100 \text{ hb} \quad , \quad G_d = 175 \text{ hb}$$

The radial load applied at the end of the cylinder was incremented by five steps of 2891 kgf. The maximal radial displacement (point 1) for the different choices of degradation factors is given in Fig. 12. It can be seen that, for the first increment, no degradation is reached for any models; for the next increment, in all cases, half of layers are degraded. After the first degradations, cases 2, 3 and 4 are stiffer than 1 because of difference in thicknesses of layers. It can be noted that case 4 (minimum degradation factor) presents a behaviour similar to multilayer element case (1) and that, for a total number of plies three times less! For all cases, spatial evolution of layer's degradation is the same. At the last increment, filaments are broken only in case 1, due to thinner geometry of plies. The curve (5) shows the linear elastic solution. Thus, if loading doesn't cause total degradation, one can reduce the number of layers (i.e., the resolution time) on using plies showing variation of angle along width.

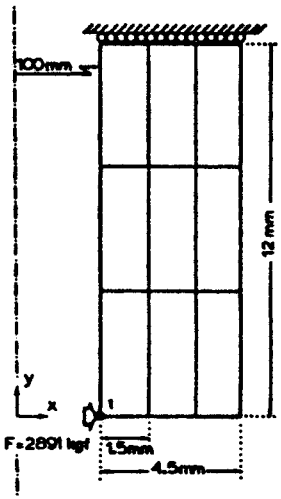

Fig. 11: Axisymmetrical cylinder discretization

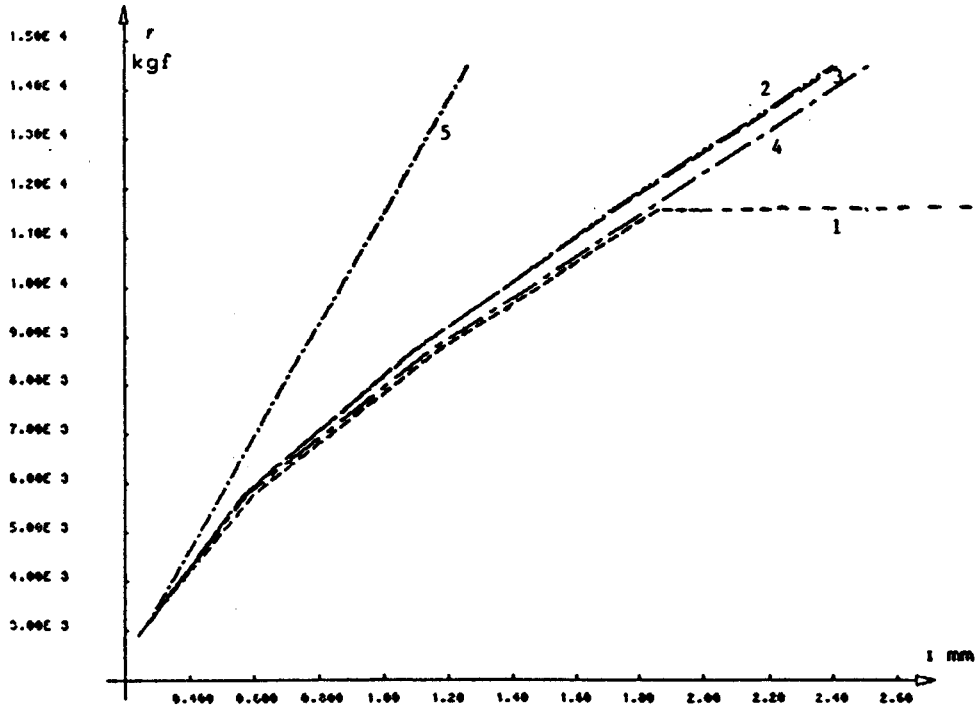

Fig. 12: Maximum radial displacement for the different models

b) Wound spherical tank

On a wound spherical tank which is a motor case of missile, we compare results given by classical element and our new model. The structure is subjected to successive incremental internal pressure up to failure. Nonlinear geometrical behaviour and material nonlinearities are combined to take into account the rotations of sections.

The structure's radius equals 230 mm. The composite tank is wound by wide plies (width = 10 mm.),

- from equatorial plane ($\theta = 0°$) with a thickness of 6 mm. and winding angle varying between 8° at interior radius and 83° at exterior radius,
- to polar zone ($\theta = 83°$) with a thickness of 7 mm.

At the interior radius, the winding angle changes from 8° to 90° between equatorial plane ($\theta = 0°$) to polar region ($\theta = 83°$).

An axisymmetrical discretization of the structure is presented in Fig. 13. The first model is formed with classical monolayer elements; the second one contains classical monolayer elements between equatorial plane ($\theta = 0°$) and $\theta = 60°$ and monolayer elements with variation of angle between $\theta = 60°$ to polar zone. Indeed, as shown on Fig. 4, it can be noted that, for $\theta < 60°$, variation of angle is less or equal to 5°: we have neglected this little variation. Structure's discretization contains 163 elements and 1121 degrees of freedom.

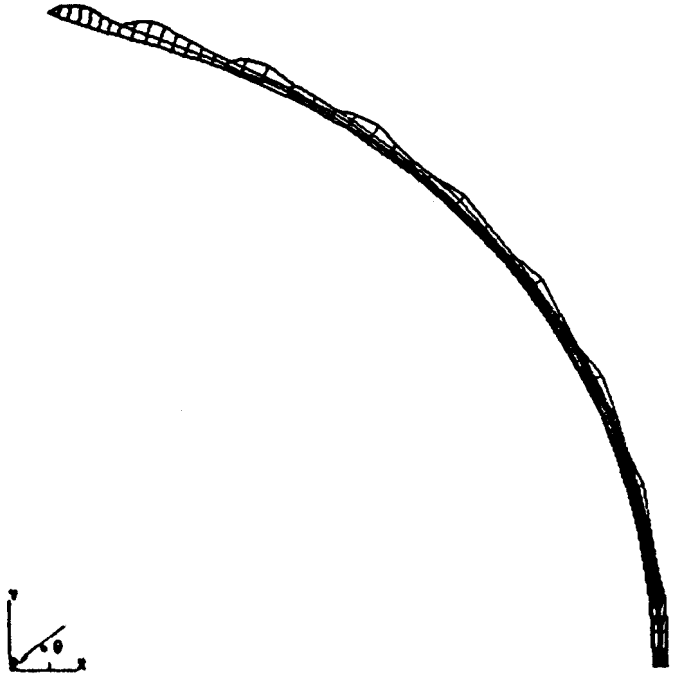

Fig. 13: Axisymmetrical discretization of wound composite tank

The material behaviour is assumed to be linear before degradation. The mechanical properties of layers follow:

$$E_1 = 16380 \text{ hb} \quad ; \quad E_2 = E_3 = 300 \text{ hb}$$

$$G_{12} = G_{13} = G_{23} = 400 \text{ hb}$$

$$\nu_{12} = \nu_{13} = \nu_{23} = 0.28$$

The Tsai-Hill failure criterion is used; strengths are

- in the fiber direction : X = 105 hb;
- in tranversal directions : Y = Z = 7 hb;
- for shear : R = S = T = 5 hb.

After matrix degradation, tranversal and shear stresses are assumed to be maintained at their values of degradation; tranversal and shear moduli are reduced to

$$E_d = 100 \text{ hb} \ , \ G_d = 175 \text{ hb}.$$

This post-degradation behaviour and important values of degraded moduli are convenient for describing wound composite structures; indeed, as there are always twilled filaments, the strength is still high after degradation. [5]

The degradation process being irreversible, one has to follow precisely strain evolution on applying little load increments. The analysis indicates a quasi-linear behaviour until internal pressure of 180 bars. After, internal pressure is incremented by six steps of 1 bar to represent the degradation evolution.

Four cases were examined:

(1) linear elastic model of the tank submitted to internal pressure of 186 bars;

(2) geometrical and material nonlinear behaviour; the degradation factor is evaluated in the mean fiber direction (see section 4);

(3) as in (2) but the degradation factor is formed as a combination of the factors in the mean and extreme filaments directions;

(4) as in (2) but the degradation factor is choosen as the minimum of the three factors.

In case (1), internal pressure is applied in one time up to 186 bars. For the three last cases, load is incremented by successive steps. Until 181 bars, those three cases have the same behaviour, very similar to the linear one: there is only a matrix degradation in an element. At 182 bars, the fourth case indicates 19 degraded elements and 46 elements with broken fibers; same instantaneous degradation process occurs at 186 bars for case (3) and at 185 bars for case (2).

As fibers directions cover all the range between 0° and 90°, all layers are well efficient until failure; the behaviour is quasi-linear until failure which occurs by instantaneous evolution of degradation in half structure.

In Fig. 14, shapes of structure under load (before failure) are presented for cases (1) and (4). Displacements are in the range of 1/10 tank thickness. Structure has a membrane behaviour in the most important part, where the thickness is constant. However, in polar region, the thickness increasing causes a local stiffening of the tank. The linear analysis doesn't take into account geometrical stiffening; then, case (1) indicates more important rotations in polar zone. Cases (2) and (3) are similar to the case (4) which predicts failure under lower pressure.

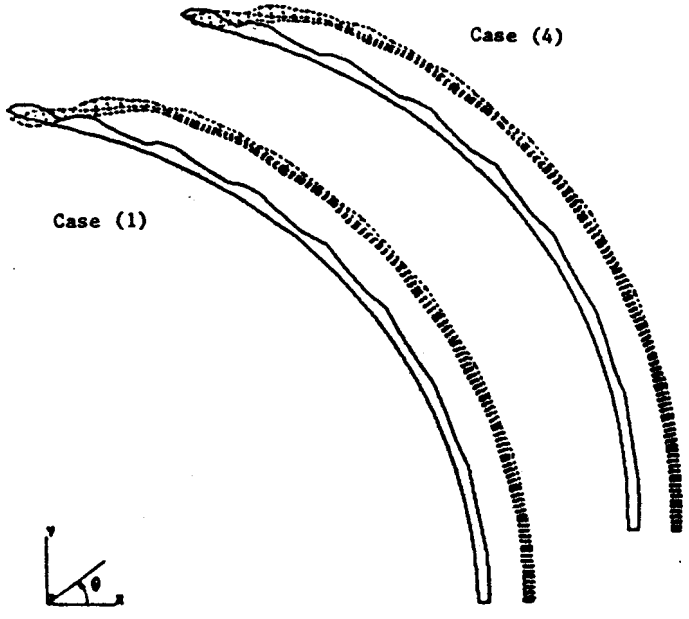

Fig. 14: Shape of structure under load

——— initial structure
------ structure under load
(1) linear analysis
(4) nonlinear geometrical and material analysis

On Fig. 15, we can see degraded elements before total failure for the fourth cases; degraded elements are localized in polar region where flexion moments are the most important (see Fig. 14). As there are few degraded elements before total failure, behaviours are little dependent of factor degradation choice.

In polar zone, stresses in extreme filament directions give bounds of a trust interval centered on stresses in mean fiber direction. In this example, the quotient $\frac{\sigma_{\alpha l}\ 11 - \sigma_{\alpha m}\ 11}{\sigma_{\alpha m}\ 11}$ where σ_{11} is longitudinal component, reaches 20% in some plies. Thus, the stresses given by classical element having fibers in uniform α_m direction, have a precision of 20%.

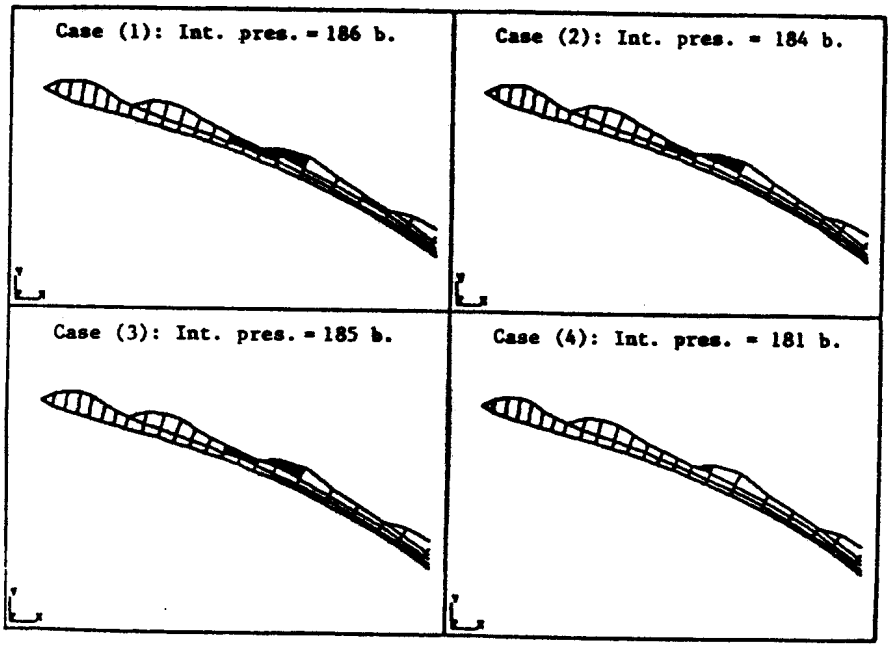

Fig. 15: Localization of degraded elements before total failure

6. Conclusions

The proposed element has been conceived in order to compare experimental and numerical results and to foresee, in numerical way, failure of wound composite structures under internal pressure. As polar zones of such revolution structures wound by wide plies are critical, it's shown, on a real example, that variation of angle along the width of a layer has to be taken into account to evaluate stresses (relative difference between stresses in mean fiber and extreme filaments directions can reach 20%!) and to decree intralaminar degradation.

Finally, to decrease the resolution cost, it can be interesting, as illustrated in the cylinder example, to consider an equivalent monolayer element with variation of fiber direction instead of classical multilayer element formed with plies having fibers in uniform direction.

REFERENCES

[1] P.R. Langston. "Kevlar aramid as a fiber reinforcement with emphasis on aircraft". Progress in Science and Engineering of Composites, ICCM IV, Tokyo, 1982, pp 1639-1672.

[2] M. Papot, Y. Grenie. "From outer space to the Great Ocean's depths: An adventure in high performance composite materials". Progress in Science and Engineering of Composites, ICCM IV, Tokyo, 1982, pp 1685-1691.

[3] S. Idelsöhn, G. Laschet and C. Nyssen. "Pre- and post-degradation analysis of composite materials with different moduli in tension and compression". Computer methods in applied mechanics and engineering, 30 (1982), pp 133-149.

[4] J.-P. Jeusette, G. Laschet. "Description d'un élément multicouche pour l'analyse des structures bobinées par nappes larges". LTAS, Rapport SF-135, University of Liege, Belgium.

[5] C. Nyssen. "Modélisation par éléments finis du comportement non linéaire des structures aérospatiales". Thèse de Doctorat, Rapport LTAS SF-86, Université de Liège, 1979.

[6] SAMCEF. "Système d'analyse des milieux continus par éléments finis". LTAS, University of Liège.